Simulation of C-Ring, O-Ring and tensile ring specimens for Iodine induced Stress Corrosion Cracking experiments on zirconium alloy

Kamila WILCZYNSKA[1, 2], Matthew BONO[1], David LE BOULCH[1], Marion FREGONESE[3], Valérie CHABRETOU[4], Nathanael MOZZANI[5], Martin RAUTENBERG[6]

[1]CEA-DEN, Service d'Études des Matériaux Irradiés, CEA, Université Paris-Saclay, F-91191, Gif-sur-Yvette Cedex, France
[2]INP Grenoble, 38031 Grenoble, France
[3]INSA de Lyon, 21 avenue Jean Capelle, 69621 Villeurbanne Cedex, France
[4]FRAMATOME 10 rue Juliette Récamier, 69456 Lyon, France
[5]EDF R&D, EDF Lab les Renardières, Avenue des Renardières – Écuelles, 77250 Moret sur Loing-Orvanne, France
[6]EDF DIPNN, 19 rue Pierre Bourdeix, 69363 Lyon, France

Abstract:

Iodine-induced stress corrosion cracking (ISCC) is a failure mechanism that can occur in nuclear fuel cladding as a result of Pellet Cladding Interaction (PCI) during incidental power transients in the reactor. This work presents an assessment of the feasibility of C-Ring, O-Ring and tensile ring specimens for ISCC experiments. The study is performed with the CAST3M finite element code, which uses viscoplasticity models developed for cold worked stress-relieved (CWSR) Zircaloy-4 fuel cladding at French Alternative Energies and Atomic Energy Commission (CEA) in order to calculate the stresses and strains in the specimens for specific types of mechanical loading. The calculated stresses and strains are subsequently used in a model that predicts the damage that occurs in the material due to stress corrosion. The damage model uses material constants that had been evaluated on the basis of previously performed experiments [T. Jezequel et al. (2017)]. This damage model predicts the time to-failure via ISCC. In addition, the CAST3M code is used to calculate the time-to-mechanical-failure of the sample, using a mechanical strain criterion. The likelihood of observing failure by ISCC rather than mechanical failure is then assessed by comparing the time-to-failure by ISCC to the time-to-mechanical-failure. The analysis was performed for C-Ring, O-Ring, and tensile ring specimens for the following cases: Applied Force and Applied Strain Rate, in both compression and tension, at 300°C, 350°C and 410°C.
In order to observe ISCC on CWSR Zircaloy-4, a C-Ring specimen requires a load in the range of 5-8 kg per cm of width of the specimen, where the width corresponds to the length in the axial direction. Tensile loads appear to be more likely to produce ISCC than compressive loads. An O-Ring specimen requires a compressive load in the range of 20-30 kg per cm of width of the specimen. Tensile ring specimens require a tensile load in the range of 60-90 kg per specimen. The results indicate that ISCC is more likely to occur at low temperatures (300-350°C) than at higher temperatures (410°C).

Keywords:
Pellet-Cladding Interaction, Iodine-Induced Stress Corrosion Cracking, C-Ring, O-Ring, Zircaloy-4.

Introduction

Pressurised Water Reactor (PWR)

Pressurized Water Reactors (PWR) use heat energy from fission of fuel atoms to produce electricity. Light water (H_2O) operates as the coolant of the reactor as well as the moderator for neutrons. A vital part of the reactor is the fuel. PWR's utilize Uranium Oxide (UO_2) pellets as the fuel. The pellets are stacked inside cladding tubes made of zirconium alloy to form rods, and 264 rods are congregated together to create a fuel assembly. A 1300 MWe core is composed of 193 fuel assemblies. Figure 1 presents the scheme of one nuclear fuel rod in the assembly with surrounding it water.

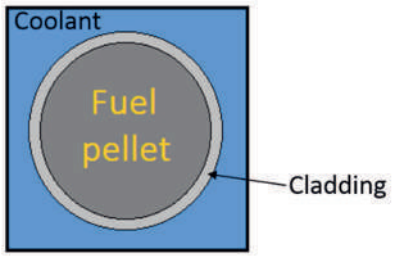

Figure 1 - Cross section of a nuclear fuel rod in the reactor

Zirconium alloys properties

Zirconium alloys are widely used in the nuclear industry as cladding material due to their good thermo-mechanical, chemical and neutronic properties. Zirconium has a high melting point, good thermal conductivity, low thermal expansion, good corrosion resistance and low cross section for capture of thermal neutrons.

Zirconium is a reactive metal with a great affinity to oxygen. When exposed to air or water (oxygen-containing environment), a protective oxide film is created on its surface. This protective oxide layer grants Zirconium alloys an excellent general corrosion resistance in many environments.

Zirconium cladding behaviour in pellet cladding interaction (PCI)

Nuclear reactors in France need to continually adjust their electricity output to follow demand hence the power of the reactor is moderated frequently. This practice is known as load following. During an increase in power, the pellet expands. Because the pellet is in contact with the cladding, the increase in its diameter is imposed on the cladding and creates a thermomechanical loading. This phenomenon is called Pellet Cladding Interaction (PCI).

Iodine is one of the fission products produced in the pellet. As it is released in gaseous form, it can move toward the cladding. Under the thermal load, the fuel expands and forms radial cracks along which the iodine can migrate towards the cladding. The thermomechanical load combined with the corrosive iodine environment may lead to ISCC. This, in turn, may lead to the fracture and failure of the cladding and the release of radioactive material into the primary water. An example of the cracking of a fuel pellet and a crack in the cladding caused by Iodine Stress Induced Cracking (ISCC) are shown on Figure 2. Both the stress that the expanding fuel imposes on the cladding and the presence of mobile, gaseous iodine create the environment necessary for ISCC to occur.

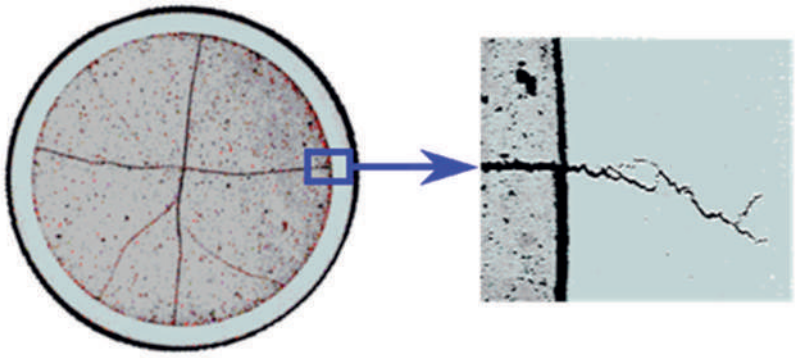

Figure 2 - ISCC crack in fuel cladding [1]

In order to reduce fuel cycle costs, advanced fuel for Light Water Reactors (LWR) is designed in a way to achieve "Zero Fuel Failure" while increasing the discharge fuel burnup. For this reason an intensified research must be focused on the properties of the materials used in the nuclear fuel rods.

Figure 3 - Pinhole cracks on the surface of Zircaloy-4 cladding tubes caused by ISCC [2]

Viscoplasticity of zirconium alloys

The PCI conditions occur during normal or incidental operation of a power plant, e.g. during power transients. The increased thermo-mechanical load on the cladding due to the expansion of the fuel causes the cladding to viscoplastically deform.

Method

Objective

The purpose of this study is to evaluate the feasibility of ISCC experiments in a chemically controlled environment, i.e. with a reduced amount of instrumentation to minimize the probability of chemical interactions between various components. To this end, several specimen designs are studied (C-Ring, O-Ring and tensile ring specimens) with the CAST3M Finite Element Modeling Code [3]. Besides, various types of loading modes are analyzed in terms of the resulting stresses and strains in the samples in order to assess the likelihood of ISCC and the time-to-failure by ISCC.

During a test, a sample can fail either due to ISCC or due to the mechanical loading only. The time required for mechanical failure of the specimen (further referred as time-to-ductile-failure) is calculated, and is defined as the time required for the specimen to reach a diametrical deformation of 40% (for C-Ring and O-Ring) or 18% (for tensile ring). The values were arbitrarily chosen based on the evolution of strain in time during mechanical loading; a sharp increase in strain rate is observed at the last phase of loading – tertiary creep. A damage model

is used to calculate the time-to-failure of the sample by ISCC, as a function of the stress in the sample and the temperature.
The objective of the study is to identify the sample geometries and loading modes that will lead to failure by ISCC, meaning that failure by ISCC occurs before mechanical failure of the sample. The specimen type and loading mode giving the best results are intended to be implemented on a new ISCC experimental setup (not developed in this paper).

Viscoplasticity model for CWSR Zircaloy-4

This model was developed in CEA by A. Soniak [4] on the basis of general viscoplastic models and aims to represent the behavior of Zircaloy-4 during PCI. The model defines an equivalent viscoplastic rate as a function of a primary viscoplastic strain rate V_p and a secondary viscoplastic strain rate V_s as:

$$\dot{\varepsilon}_{eq}^{vp} = V_s + \left((V_p - V_s).exp\left(-\frac{\varepsilon_{eq}^{vp}}{\varepsilon_0}\right)\right) \quad (1)$$

The viscoplasticity of the Zy4 reaches its secondary regime when the viscoplastic equivalent strain bigger than ε_0.
The primary and the secondary strain rates are written as a function of the temperature T, the Hill stress and the neutronic fluence $\emptyset_t$ as follows:

$$V_p = V_{p0}(\sigma_{Hill}, T).V_{pf}(\emptyset_t) \quad (2)$$

$$V_s = V_{s0}(\sigma_{Hill}, T).V_{sf}(\emptyset_t) \quad (3)$$

The orthotropy of the Zy-4 is taken into account through the use of the Hill stress in the model. Above model is used to estimate the time to-ductile-failure, where the failure of the specimen occurs due to the mechanical loading. The failure of the specimen is defined as its diametrical deformation of 40% (for C-Ring and O-Ring) or 18% (for tensile ring).

Kachanov damage model

This model was developed on the basis of the work of L. Kachanov [5]. It is used to estimate a time-to-initiate an ISCC crack of the sample in [2] and can be described by Eq. (4) and Eq. (5).

$$\frac{dD}{dt} = A\,(\frac{\sigma}{1-D} - \sigma_0)^n \quad (4)$$

$$A = A_0 e^{(\frac{-T_0}{T})} \quad (5)$$

D is the damage variable, T_0, n, A_0 are the material parameters determined by fitting the calculated times to failure to the experimental results of ISCC creep tests carried out in one of the previous experiments, σ_0 is an ISCC threshold Hoop stress, $\sigma/(1-D)$ constitutes as an effective Hoop stress, t is the time and T is the temperature.
The hoop stress threshold σ_0 for ISCC was estimated as 240-290 MPa based on internal pressure creep tests on cladding samples [2]. The study suggests that the hoop stress threshold is independent of the temperature between 320°C and 380°C [2].
The model uses the scalar variable D to represent material damage. Initially D is set to 0, since no damage has occurred. With time, the damage due to ISCC progresses, and the value of D approaches 1. Upon reaching a value of 0.995 (arbitrary chosen close to 1) the inner surface of the cladding is assumed to be damaged to the extent that a crack initiates. Since

the initiation time of an ISCC crack is significantly greater that the propagation time ([6], [7] and [8]) the time-to-rupture is assumed to be approximately equal to the crack initiation time. As a consequence, the time-to-initiate an ISCC crack calculated with the Kachanov's model is assumed to be the same as the time-to-failure. Following this assumption, the parameters of the un-irradiated CWSR Zy-4 were identified in [2]. As in [2], the model is applied in the post-treatment of the calculation results, where the time-to-rupture is calculated based on the local hoop stress values at a chosen point in the cladding.
The model is solved in post-treatment using a Runge-Kutta method available in CAST3M. Above model is used to estimate the ISCC time-to-failure, where the failure of the specimen occurs due to the ISSC.
In the paragraphs below, the ISCC time-to-failure will be compared to the time-to-ductile-failure defined before.

Finite-Element Modelling (FEM) with CAST3M

The calculations were performed for three specimen geometries: C-Ring, O-Ring and tensile ring. The specimen was converted into a 2-dimensional model. Figure 4 presents the model for the C-Ring. The simulated C-Ring has an outer radius of 4.75 mm and thickness of 0.570 mm. Figure 5 presents the model for the O-Ring. The simulated O-Ring has the same dimensions as previously stated C-Ring. For calculations using tensile loads applied, a tensile ring geometry presented on the Figure 6 was used, where the width of the gage section of the sample is 2 mm.
For the simulation of the O-Ring, vertical rigid body motion was implemented for the platen. For the simulation of the tensile ring, vertical rigid body motion was implemented for the mandrel. Moreover, an assumption was made that the contact of the platen or the mandrel with the sample (transition of the load) is frictionless (friction coefficient = 0).
The orthotropy of the cladding is defined in the radial-tangential-axial referential of the cladding. It is defined on the initial geometry and is not updated all along the calculation.

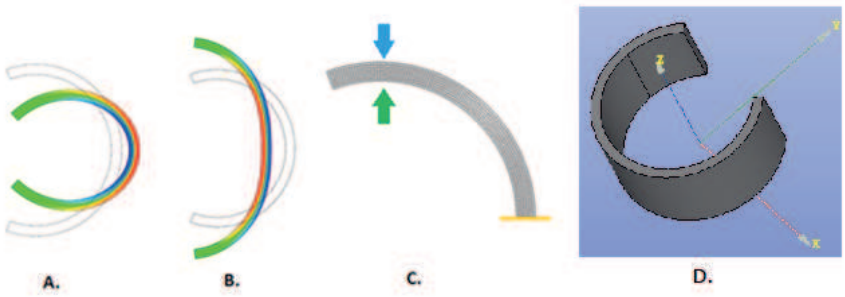

Figure 4 - Model for a C-Ring specimen: A. deformation in compression, B. deformation in tension, C. actual simulated geometry, where blue arrow indicates the load direction applied during compression and green one the load direction applied during tension. Moreover, orange line shows the symmetry plane used during calculation, D. 3-D model of the sample.

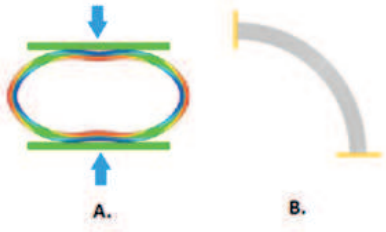

Figure 5 - Model for an O-Ring specimen: A. deformation in compression, B. actual simulated geometry. Blue arrows indicate the load direction applied during compression. Moreover, orange lines show the symmetry plane used during calculation.

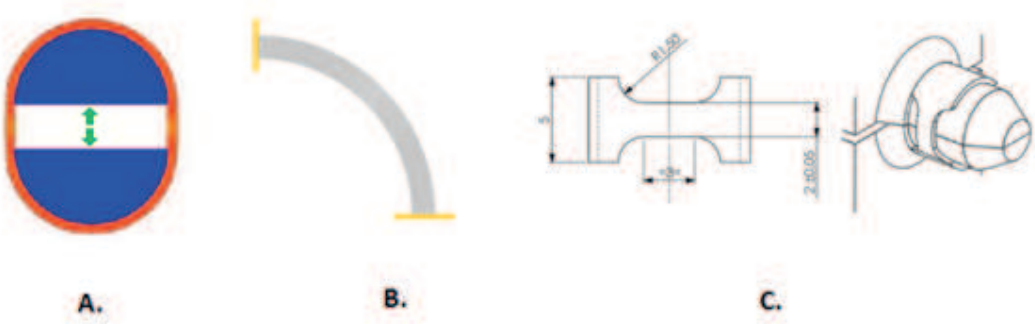

Figure 6 - Model of the tensile ring specimen used in a ring tensile test: A. deformation in tension, B. actual simulated geometry (the mesh of the mandrel is not displayed). C. tensile ring specimen scheme. Green arrows indicate the load direction applied during tension. Moreover, orange lines show the symmetry plane used during calculation.

The calculations were performed in 2D within the plane strain assumption, adopting large displacements method (the geometry is updated during the calculation). The loads consist in applying a constant force or a constant strain rate to the specimen, in tension (for the C-Ring and the tensile ring specimen) or in compression (for the C-Ring and the O-Ring specimen). Homogeneous and constant temperatures of 300°C, 350°C or 410°C were maintained throughout the calculation.

The deformation of the specimen is defined as: $\varepsilon = \frac{(H-H_0)}{H_0}$, where H is the initial height of the specimen and H_0 is the height of the deformed specimen due to the loading. Figure 7 presents how the deformation is defined for the investigated specimens. The mechanical failure occurs upon reaching a deformation of 40% (for C-Ring and O-Ring) and 18% (for tensile ring). This condition defines the "ductile failure" of the specimen described before and leads to an evaluation of the time-to-ductile-failure. It defines also a condition to stop the FEM calculations and is the final simulated time. In the calculations, the final simulated time cannot be longer than 100 hours.

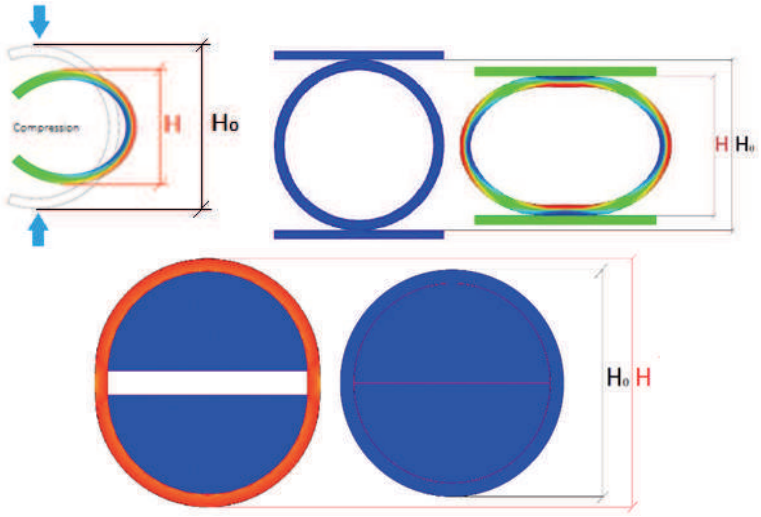

Figure 7 - Definition of mechanical failure for C-Ring, O-Ring and tensile ring (with the mandrel) respectively. Deformation of a specimen is defined as: $\varepsilon = \frac{(H-H_0)}{H_0}$.

Results

For each C-Ring, O-Ring and tensile ring specimens, the analysis was performed for the following cases: Force Applied, and Strain Rate Applied in either compression or tension for 300°C, 350°C and 410°C. The strain rate is defined as the change of deformation in time: $\frac{d\varepsilon}{dt}$. The values of the Strain Rate Applied were chosen as follow: 10^{-4}, 10^{-5}, and 10^{-6} s^{-1}, which corresponds to the strain rates that the cladding may be exposed to during power transients in a nuclear reactor.

The presented results include graphs of the evolution of the local Hoop Stress as a function of time for chosen cases. The paragraphs below refer to the hoop stress on the plane of symmetry of the sample. The maximum tensile stress can occur either at the inner surface or the outer surface of the sample, depending on the sample type and loading mode.

For chosen cases, a table presents the calculated time-to-ductile-failure and the calculated ISCC time-to-failure. Moreover, a ratio (r) of time-to-ductile-failure to ISCC time-to-failure is calculated in order to assist in the analysis.

$$r = \frac{time\ to\ ductlie\ failure}{time\ to\ ISCC\ failure} \tag{12}$$

In the tables the following terms are used:

- YES (if r > 1.5) – ISCC is expected to be observed on the specimen.
- NO (if r < 1.0) – ISCC is not expected to be observed on the specimen.
- Not certain (if 1.5 ≥ r > 1) – ISCC may or may not be observed on the specimen, and the results are not conclusive.

Zr-4 C-Ring Force imposed

The loads are defined as an applied weight per unit of width of the cladding (in kg/cm). The width of the specimen corresponds to its length in the axial direction of the cladding.

Figure 8 shows the evolution of the stress in time and of the bending moment in time. The bending moment is evaluated in the thickness of the cladding, on the symmetry plane of the specimen. The hoop stress is evaluated at the inner wall of the cladding for the tensile loads and at the outer wall of the cladding for the compressive loads respectively.

First phase (rapid increase of the stress and bending moment) is the phase where the load is applied (loading phase). Then the stress evolves due to the combined effect of viscoplasticity of the material and deformation of the structure. The viscoplasticity tends to relax the stresses (see Figure 9) while the deformation of the structure will either increase or decrease the bending moment, depending on if the load is compressive or tensile. The increase of the bending moment counteracts the viscoplastic relaxation of the stress in compression, while the decrease of the bending moment and the viscoplastic relaxation both tend to reduce the stress in tension.

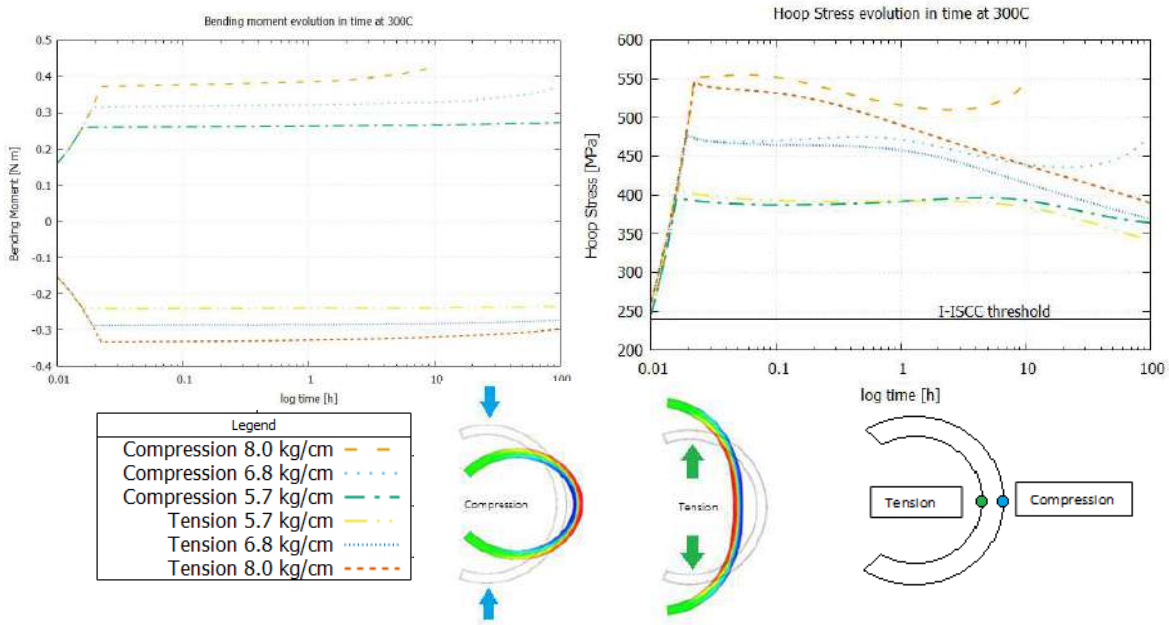

Figure 8 - Evolution of the bending moment and Hoop stress for force imposed at 300°C on Zircaloy-4 C-Ring.

The load applied to the C-Ring specimen is a bending moment in its thickness, on its symmetry plane. This bending moment results into a non-homogeneous profile of hoop stress in the thickness of the sample. Figure 9 presents this profile calculated on the symmetry plane. It can be seen that there is a gradient of the stress values along the thickness in the sample. This example presents the sample in tension. The inner wall of the cladding is in tension whereas the outer wall of the sample is in compression. Figure 9 also illustrates the effects of the viscoplasticity. After loading the sample, the level of stresses reaches its maximum. Then, given that the load is kept constant, the stresses in the sample relax, and at the same time the geometry of the sample changes such that the bending moment decreases, which result in a decrease of the level of stress. It is caused by the viscoplasticity of the material which is dependent on the temperature. The greater the temperature of the sample, the quicker the stresses decrease.

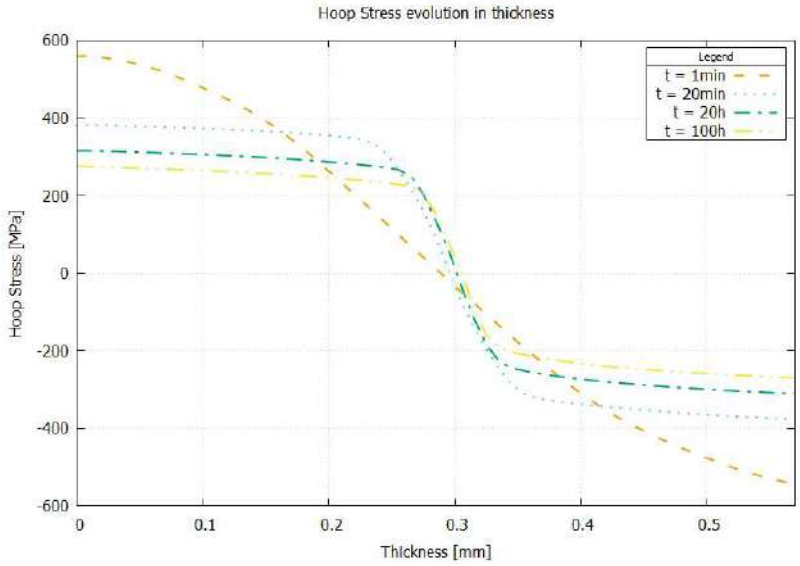

Figure 9 - Hoop stress evolution along the thickness of the C-Ring specimen (tensile load applied).

Figure 10 presents the results of the simulation for constant force applied (8.0-5.7 kg/cm) in both compression and tension for 300°C, 350°C and 410°C respectively. The calculations show that the higher the temperature the lower the level of stress and the quicker the stresses relax.

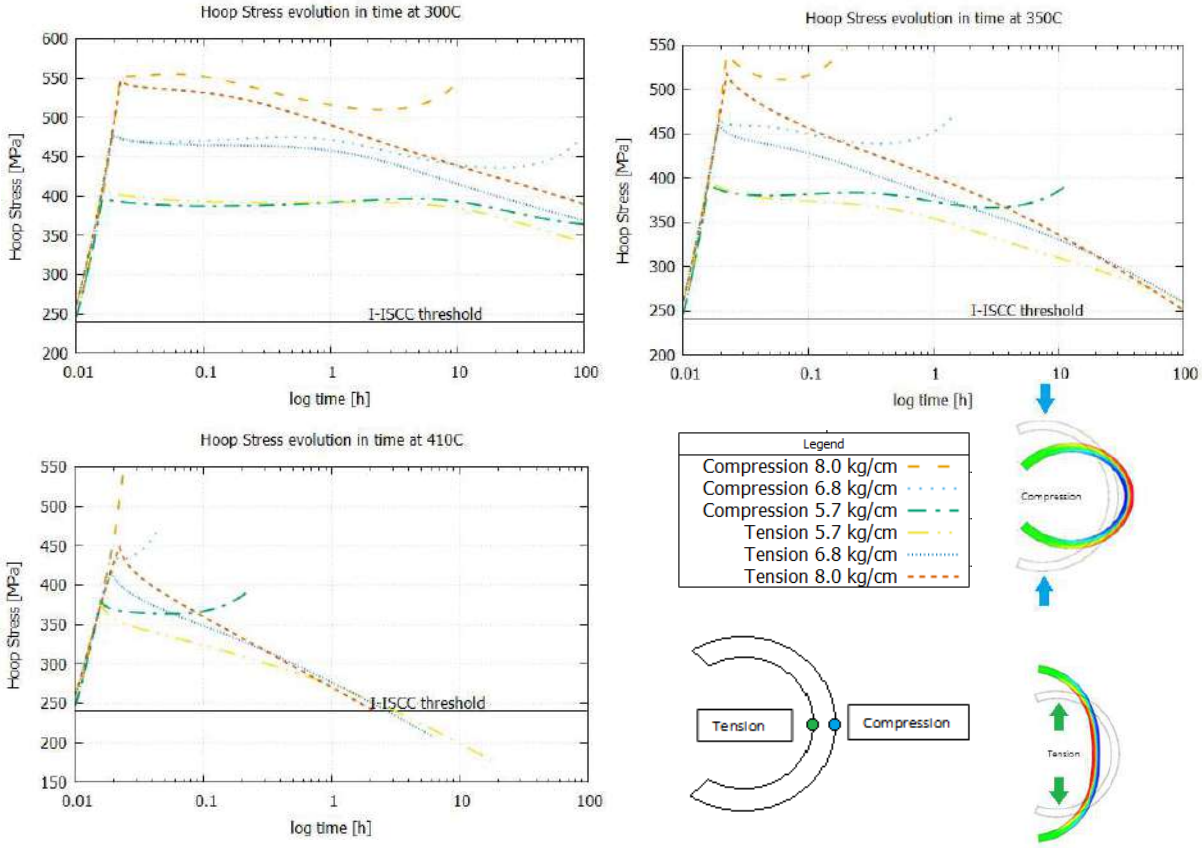

Figure 10 - Hoop stress evolution in time: Comparison of the results for different values of constant force applied at 300°C, 350°C and 410°C on Zircaloy-4 C-Ring.

Table 1 presents the assessment of the use of the C-Ring in ISCC experiment for values of constant force applied. The ISCC-time-to-failure are compared with the time-to-ductile-failure. Using tensile loads ranging from 5.7-8.0 kg/cm, the ISCC-times-to-failure are significantly lower than the times-to-ductile-failure, at all the studied temperatures. This result suggests that ISCC should be observable with tensile C-Rings at those temperatures. Using compressive loads ranging from 5.7-8.0 kg/cm at 410°C the specimen should lead to almost immediate failure of the specimen due to the mechanical loading only. For compressive load of 8.0 and 6.8 kg/cm at 410°C, the ductile failure due to the mechanical loading only occurs immediately resulting in the value of calculated the time-to-ductile failure lower than 0.1h. In those cases the damage model used for the estimation of ISCC-time-to-failure did not evaluate any crack failure in the calculation, which can be seen by the lack of the ISCC-time-to failure value.

Table 1 - Assessment of the use of Zircaloy-4 C-Ring in ISCC experiment for different values of constant force applied at 300°C, 350°C and 410°C.

Character of load	**Compression**			**Tension**		
Load applied [kg/cm]	**8.0**	**6.8**	**5.7**	**5.7**	**6.8**	**8.0**
	Temperature 300°C					
Time-to-ductile-failure [h]	10.1	89.7	>100	>100	>100	>100
ISCC Time-to-failure [h]	1.2	1.9	4.1	4.3	2.1	1.4
ISCC {ratio}	YES 8.4	YES 46.7	YES >24.6	YES >23.5	YES >49.7	YES >72.5
	Temperature 350°C					
Time-to-ductile-failure [h]	0.2	1.4	11.7	>100	>100	>100
ISCC Time-to-failure [h]	-	0.5	0.9	1.2	0.6	0.4
ISCC {ratio}	NO -	YES 2.8	YES >13	YES >83.3	YES >167	YES >250
	Temperature 410°C					
Time-to-ductile-failure [h]	<0.1	<0.1	0.2	18.1	6.1	2.2
ISCC Time-to-failure [h]	-	-	0.2	0.5	0.2	0.2
ISCC {ratio}	NO -	NO -	NO 1	YES 36.2	YES 30.5	YES 11

Zr-4 C-Ring Strain rate imposed

In this paragraph, the load is defined as a deformation rate imposed on a specimen, which is given by the displacement applied to the sample divided by the initial outer diameter of the cladding (see Figure 7).

Figure 11 shows the results of the simulation for constant strain rate applied for temperatures 300°C, 350°C and 410°C respectively. The calculations for 300°C and 350°C show that the calculated hoop stress is higher than the hoop stress threshold. It can be observed that, at 410°C, a strain rate of 10^{-6} s^{-1} is too slow and the hoop stresses is too low for ISCC to occur. It can also be concluded that the level of stresses is slightly higher for tensile loading than for compressive loading. This suggests that loading the sample in tensile is more likely to produce ISCC.

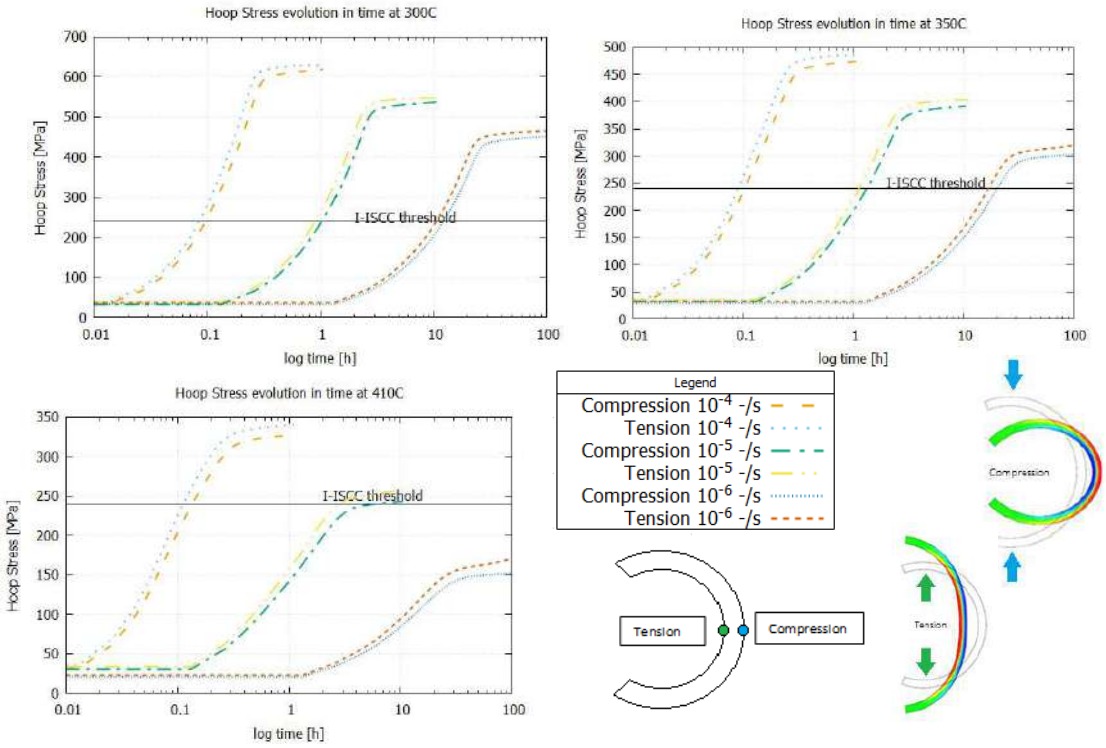

Figure 11 - Hoop stress evolution in time: Comparison of the results for different values of constant force strain rate at 300°C, 350°C and 410°C on Zircaloy-4 C-Ring.

Table 2 presents the assessment of the use of the C-Ring in ISCC experiment for values of constant strain rate applied. It can be seen in all temperatures examined it should be possible to observe ISCC before purely mechanical ductile failure only using the highest tensile strain rate, 10^{-4} s^{-1}. Moreover, the best temperature for observing ISCC is 350°C, where the use of all investigated loads should lead to the observation of ISCC.

Table 2 - Assessment of the use of Zircaloy-4 C-Ring in ISCC experiment for different values of constant strain rate applied at 300°C, 350°C and 410°C.

Character of load	**Compression**			**Tension**		
Strain rate applied [s^{-1}]	**10^{-4}**	**10^{-5}**	**10^{-6}**	**10^{-4}**	**10^{-5}**	**10^{-6}**
	Temperature 300°C					
Time-to-ductile-failure [h]	1.06	10.6	>100	1.11	11.1	>100
ISCC Time-to-failure [h]	0.90	3.4	23.8	0.82	3.0	21.1
ISCC {ratio}	Not certain 1.2	YES 3.2	YES >4.2	Not certain 1.35	YES 3.7	YES 4.7
	Temperature 350°C					
Time-to-ductile-failure [h]	1.06	10.6	>100	1.11	11.1	>100
ISCC Time-to-failure [h]	0.58	3.3	33.0	0.51	2.9	27.7
ISCC {ratio}	YES 1.9	YES 3.2	YES 3	YES 2.2	YES 3.8	YES 3.6

	Temperature 410°C					
Time-to-ductile-failure [h]	1.06	10.6	>100	1.11	11.1	>100
ISCC Time-to-failure [h]	0.73	-	-	0.59	-	-
ISCC {ratio}	Not certain 1.45	NO -	NO -	YES 1.86	NO -	NO -

Zr-4 O-Ring Force imposed

The loads are defined as an applied weight per unit of width of the cladding (in kg/cm). The width of the cladding corresponds to its length in the axial direction.

In the case of an O-Ring specimen, a rapid decrease in hoop stress occurs after a certain deformation. The decrease in stress is caused by the decrease of the bending moment (Figure 13). This is a structural effect of the O-Ring loaded with the use of platens. There is initially a single point of contact between each platen and the specimen. As the specimen deforms, its shape changes and it causes the creation of two points of contact (Figure 14). It is possible to avoid this effect by using another type of loading, e.g. the one proposed by R.W. Bosch et al. in [9]. In that concept, the O-Ring specimen is loaded by 4 rods (see Figure 15).

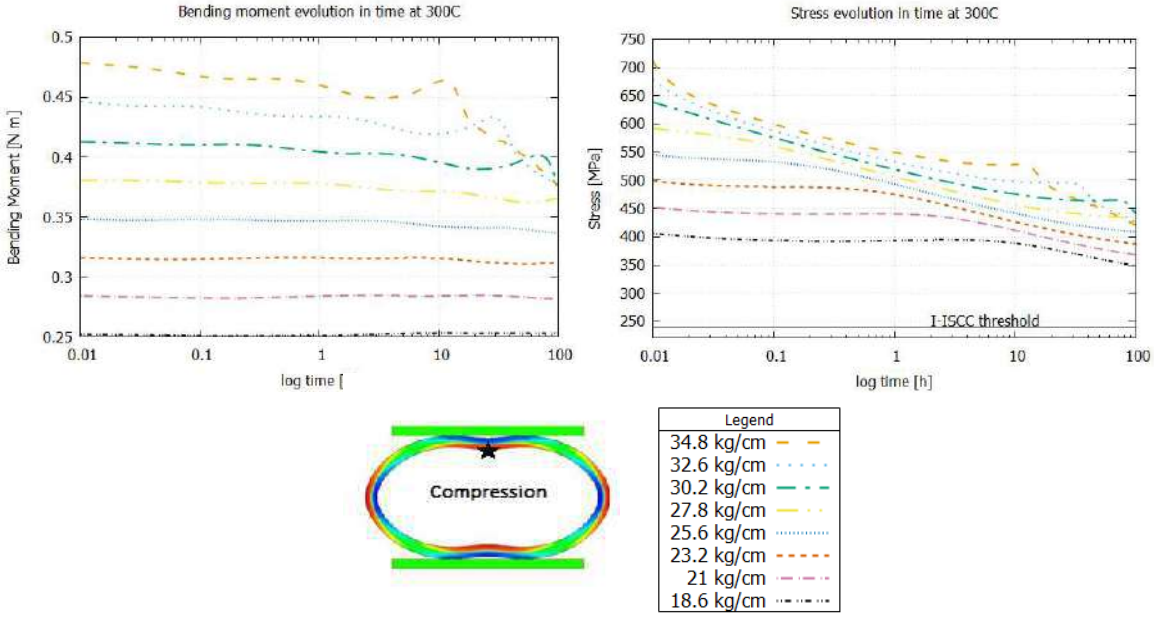

Figure 13 - Evolution of the bending moment and Hoop stress for force imposed at 300°C on Zircaloy-4 C-Ring.

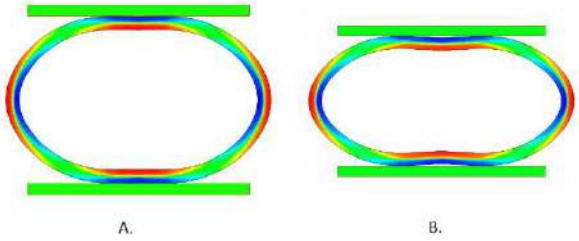

Figure 14 - O-Ring loading by platen, where A. one point of contact between specimen and platen and B. two points of contact between specimen and platen.

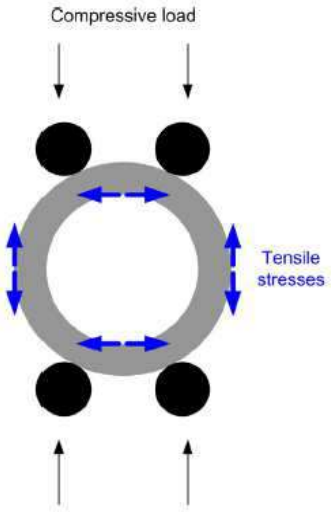

Figure 15 - O-Ring loading by 4 rods [9]

Figure 16 shows the results of simulation for constant compressive force applied (34.8 -18.6 kg/cm) for 300°C, 350°C and 410°C. ISCC should be observed in all temperatures only applying the compressive force in the range 27.8 -18.6 kg/cm. Table 3 presents the assessment of O-Ring applicability for abovementioned cases.

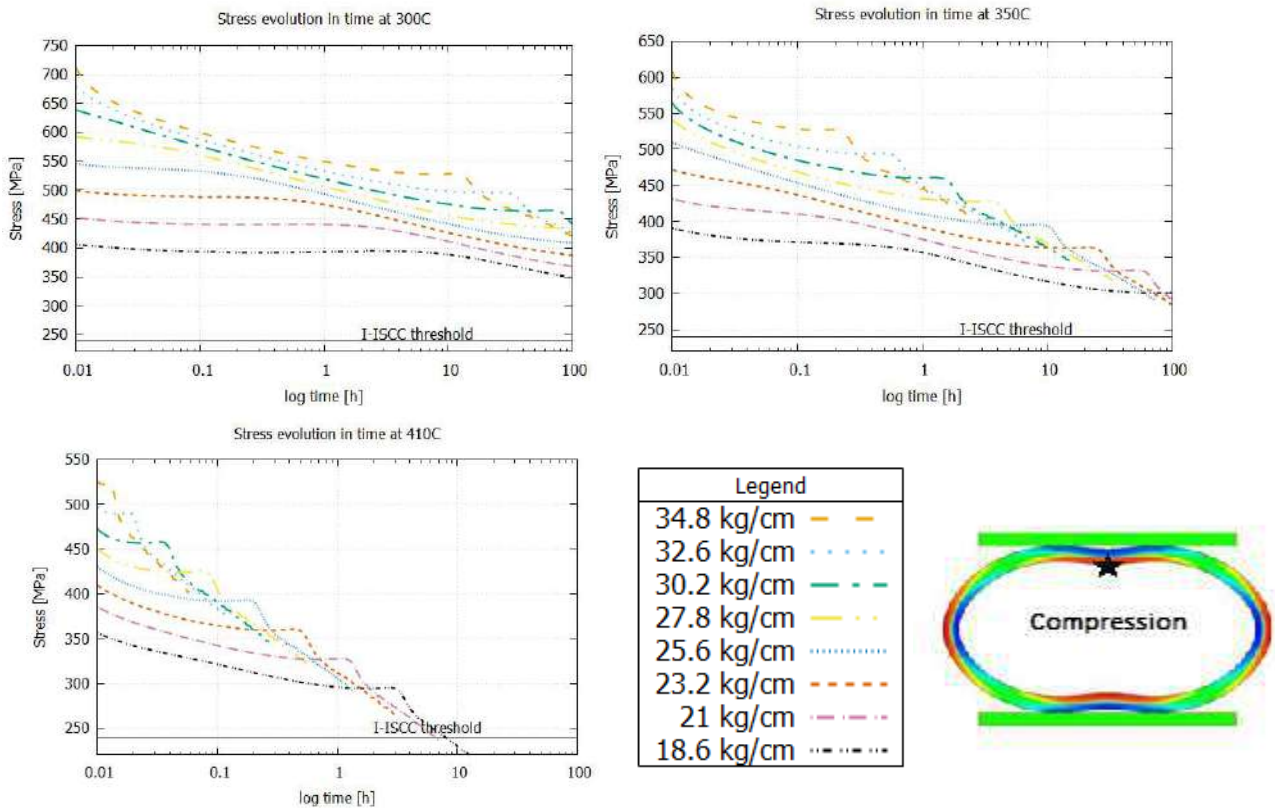

Figure 16 - Hoop stress evolution in time: Comparison of the results for different values of compressive constant force applied at 300°C, 350°C and 410°C on Zircaloy-4 O-Ring.

Table 3 - Assessment of the use of Zircaloy-4 O-Ring in ISCC experiment for different values of constant compressive force applied at 300°C, 350°C and 410°C.

Character of load	**Compression**							
Load applied [kg/cm]	34.8	32.6	30.2	27.8	25.6	23.2	21.0	18.6
	Temperature 300°C							
Time-to-ductile-failure [h]	>100	>100	>100	>100	>100	>100	>100	>100
ISCC Time-to-failure [h]	0.8	0.9	1.0	1.2	1.4	1.7	2.4	4.1
ISCC	YES	YES	YES	YES	YES	YES	YES	YES
{ratio}	>125	>111.1	>23.8	>83.3	>71.4	>58.8	>41.7	>23.4
	Temperature 350°C							
Time-to-ductile-failure [h]	2.9	6.6	15.2	33.9	73.0	>100	>100	>100
ISCC Time-to-failure [h]	0.21	0.25	0.29	0.35	0.43	0.53	0..71	1.19
ISCC	YES	YES	YES	YES	YES	YES	YES	YES
{ratio}	13.8	26.4	52.4	96.9	169.8	>188.7	>140.8	>84
	Temperature 410°C							
Time-to-ductile-failure [h]	<0.1	0.12	0.27	0.61	1.38	3.11	6.99	15.6
ISCC Time-to-failure [h]	-	-	-	0.11	0.13	0.19	0.29	0.53
ISCC	NO	NO	NO	YES	YES	YES	YES	YES
{ratio}	-	-	-	5.5	10.6	16.4	24.1	29.4

Zr-4 O-Ring Strain-rate imposed

In this paragraph, the load is defined as a deformation rate imposed on a specimen, which is given by the displacement applied to the sample divided by the initial outer diameter of the cladding (see Figure 7).

Figure 17 shows the results of a constant strain-rate (10^{-4}, 10^{-5} and 10^{-6} s^{-1}) applied to an O-Ring specimen. Table 4 presents the assessment of the applicability of the abovementioned cases for ISCC experiments. All the compressive strain rates applied are expected to lead to ISCC, except the lowest one at 410°C. ISCC is predicted to occur more readily at 350°C for the investigated loads.

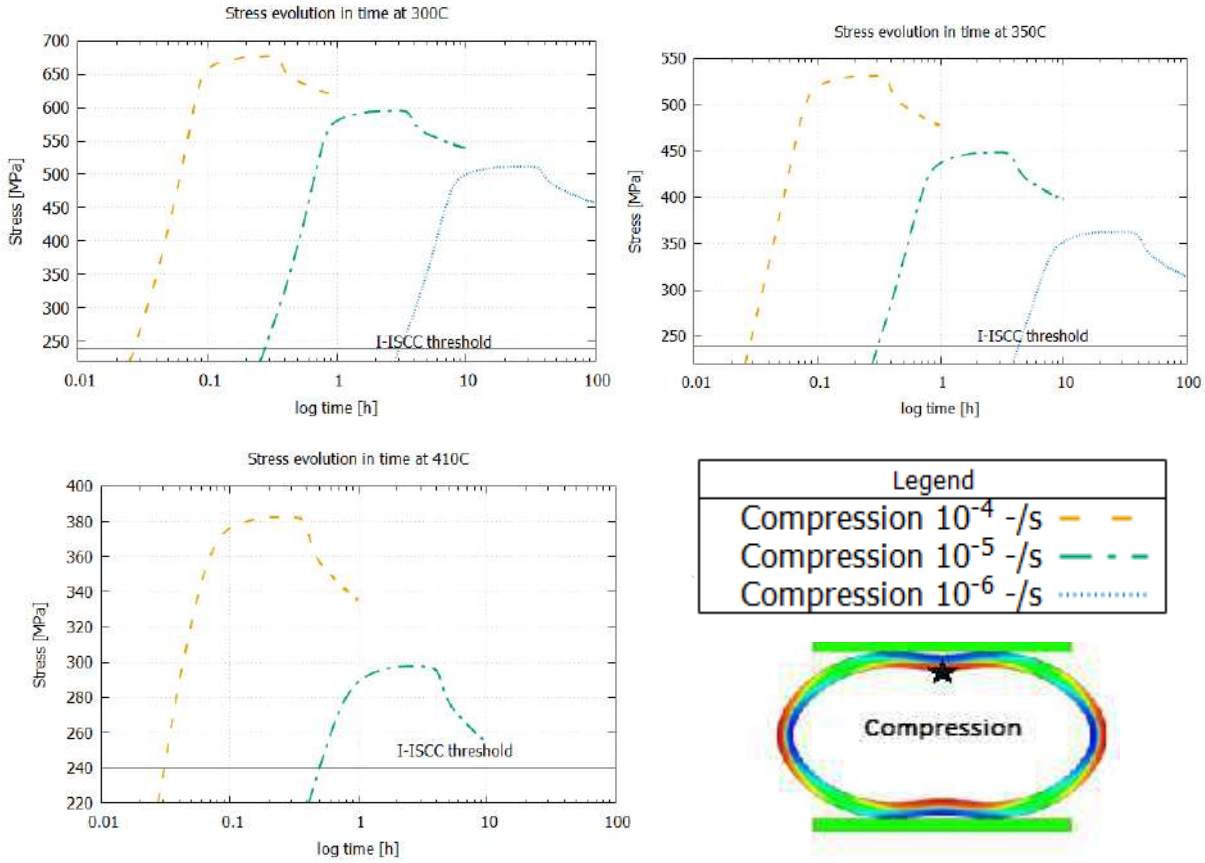

Figure 17 - Hoop stress evolution in time: Comparison of the results for different values of compressive constant strain-rate applied at 300°C, 350°C and 410°C on Zircaloy-4 O-Ring.

Table 4 - Assessment of the use of Zircaloy- 4 O-Ring in ISCC experiment for different values of constant strain-rate applied, in compression, at 300°C, 350°C and 410°C.

Strain rate applied [s^{-1}]	**10^{-4}**	**10^{-5}**	**10^{-6}**
	Temperature 300°C		
Time-to-ductile-failure [h]	1	10.0	99.4
ISCC Time-to-failure [h]	0.8	5.3	26.4
ISCC {ratio}	Not certain 1.25	YES 1.89	YES 3.77
	Temperature 350°C		
Time-to-ductile-failure [h]	1	10	99.4
ISCC Time-to-failure [h]	0.53	5.3	26.4
ISCC {ratio}	YES 1.89	YES 1.89	YES 3.77

	Temperature 410°C		
Time-to-ductile-failure [h]	1	9.9	>100
ISCC Time-to-failure [h]	0.53	7.9	-
ISCC {ratio}	YES 1.89	Not certain 1.25	NO -

Zr-4 tensile ring force imposed

A tensile load is applied to a sample with a specific geometry, as shown at the bottom of Figure 18. The sample contains a gage section with a width of 2 mm and a length of 3 mm. A special mandrel, which consists of two D-shaped components, is fitted to the inner diameter of the sample. When the D-shaped components are pulled apart, the gage section of the sample is subjected to a tensile force. Unlike the cases discussed above, in which a bending moment is created in a C-Ring or in an O-Ring, the ring tensile specimen is subjected to a tensile stress throughout the cross-section.

Figure 18 shows the results of simulations for constant tensile forces applied (93.0 – 60.4 kg) at 300°C, 350°C and 410°C. Table 5 presents the assessment of the applicability of the ring tensile test the for abovementioned cases. ISCC is expected to occur at every temperature for tensile loads ranging from 83.6 - 60.4 kg. In order to avoid numerical problems that originate form large strains in the calculation, here, the time-to ductile-failure was evaluated with critical deformation equal to 18% instead of 40%.

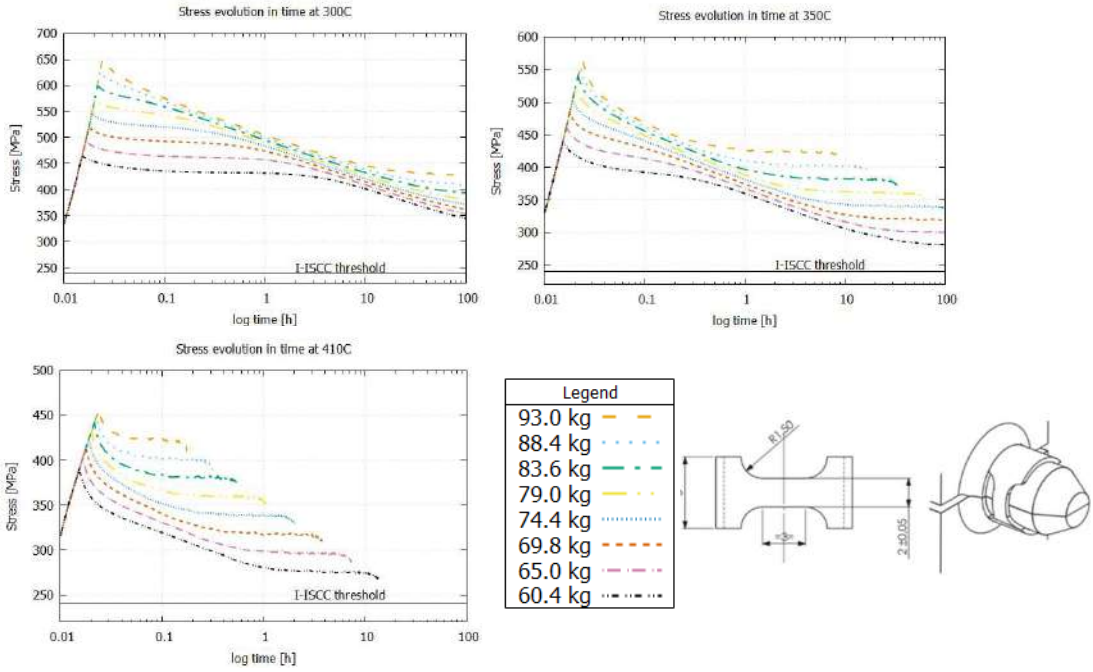

Figure 18 - Hoop stress evolution in time: Comparison of the results for different values of tensile constant force applied at 300°C, 350°C and 410°C on Zircaloy-4 ring tensile test.

Table 5 -Assessment of the use of Zircaloy- 4 ring tensile test in ISCC experiment for different values of constant tensile force applied at 300°C 350°C and 410°C.

Character of load	**Tension**							
Load applied [kg]	**93.0**	**88.4**	**83.6**	**79.0**	**74.4**	**69.8**	**65.0**	**60.4**
	Temperature 300°C							
Time-to-ductile-failure [h]	>100	>100	>100	>100	>100	>100	>100	>100
ISCC Time-to-failure [h]	1.2	1.2	1.2	1.2	1.4	1.6	1.7	2.1
ISCC	YES	YES	YES	YES	YES	YES	YES	YES
{ratio}	>83.3	>83.3	>83.3	>83.3	>71.4	>62.5	>58.8	>47.6
	Temperature 350°C							
Time-to-ductile-failure [h]	4.9	9.3	17.6	33.3	62.6	>100	>100	>100
ISCC Time-to-failure [h]	0.35	0.36	0.4	0.44	0.48	0.54	0.62	0.74
ISCC	YES	YES	YES	YES	YES	YES	YES	YES
{ratio}	14	25.8	44	75.7	130.4	>185.2	>161.3	>135.1
	Temperature 410°C							
Time-to-ductile-failure [h]	0.10	0.18	0.31	0.57	1.07	2.02	3.84	7.27
ISCC Time-to-failure [h]	-	0.12	0.14	0.16	0.20	0.24	0.32	0.42
ISCC	NO	Not certain	YES	YES	YES	YES	YES	YES
{ratio}	-	1.5	2.21	3.6	5.4	8.4	12	17.3

Conclusions

The purpose of this study is to evaluate the feasibility of ISCC experiments in a chemically controlled environment, i.e. with a reduced amount of instrumentation to minimize the probability of chemical interactions between various components. To this end, several specimen designs were studied (C-Ring, O-Ring and tensile ring specimens)

The C-Ring geometry has proven to have interesting properties. This geometry seems to be the most convenient one to achieve a significant ISCC activation with a minimum amount of instrumentation. The applied load creates a bending moment in which a tensile stress is formed on one surface of the tube and a compressive stress is formed on the opposite surface. Thus a relatively small force of only a few kg/cm can produce a large tensile hoop stress at a particular point on either the inside or the outside surface of the tube.

The O-Ring geometry should exhibit ISCC more easily than the C-Ring geometry. But it requires the use of higher loads in comparison with the C-Ring. In order to obtain ISCC using an O-Ring specimen, it is necessary to use a compressive force of 20 to 30 kg/cm: this would imply a more complex instrumentation, comparing with the C-ring case.

A ring tensile test should exhibit ISCC more easily than C-Rings and O-Ring specimen. But, it requires a load of 60 to 80 kg in order to obtain ISCC.

The calculations performed in this study indicate that ISCC is more likely to occur at low temperatures (300-350°C) than at higher temperatures. At higher temperatures, the viscoplasticity of the material leads to reduced stresses that make it more difficult to obtain ISCC.

For CWSR Zircaloy-4, both specimen geometries, loaded in either tension or in compression, are expected to produce sample failure by ISCC. In general, tensile loads appear to be more likely to produce ISCC than compressive loads.

References

1. Davies, J.H., Rosenbaum, H.S., Armijo, J.S., Proebstle, R.A., Rowland, T.C., Thompson, J.R., Esch, E.L., Romeo, G., & Rutkin, D.R. (1977). Irradiation tests to characterize the PCI failure mechanism. United States: American Nuclear Society.
2. Jezequel T., Auzoux Q., Le Boulch D., Bono M., Andrieu E., Blanc C., Chabretou V., Mozzani, N., Rautenberg M., Stress corrosion crack initiation of Zircaloy-4 cladding tubes in an iodine vapor environment during creep, relaxation, and constant strain rate tests. (2018) Journal of Nuclear Materials, vol. 499. pp. 641-651. ISSN 0022-3115
3. http://www-cast3m.cea.fr/, CEA.
4. Soniak A., L'Hullier N., Mardon J.-P., Rebeyrolle V., Bouffioux P., Bernaudat C., Irradiation Creep Behavior of Zr-base alloys, Zirconium in the Nuclear Industry thirteenth international symposium, 2002: pp. 837–862.
5. Kachanov L., Rupture Time Under Creep Conditions. International Journal of Fracture 97 : XI-XVIII, 1999.
6. Cox B., Pellet-clad interaction (PCI) failures of zirconium alloy fuel cladding – A review, J. Nucl. Mater. 172 (1990) 249-292.
7. Le Boulch D., Fournier L., Sainte Catherine C., Testing and modelling iodine induced stress corrosion cracking in stress relieved Zircaloy-4, in: Int. Semin. Pellet-Cladding Interact. Water React. Fuels, Aix-en-Provence, 2004.
8. Schuster I., Lemaignan C., Characterization of Zircaloy corrosion fatigue phenomena in an iodine environment: Part I: Crack growth, J. Nucl. Mater. 166 (1989) 348-356.
9. Bosch R.W., Vankeerberghen M., Gerard. R., Somville F., Crack Initiation Testing of Thimble Tube Material Under PWR Conditions to Determine a Stress Threshold for IASCC, Journal of Nuclear Materials 461 (2015) 112-121.